

# Journal Pre-proof

Effect of yerba mate extract on the performance of starch films obtained by extrusion and compression molding as active and smart packaging

Rocío L. Ceballos, Oswaldo Ochoa-Yepes, Silvia Goyanes, Celina Bernal, Lucía Famá



PII: S0144-8617(20)30669-X

DOI: <https://doi.org/10.1016/j.carbpol.2020.116495>

Reference: CARP 116495

To appear in: *Carbohydrate Polymers*

Received Date: 10 December 2019

Revised Date: 21 May 2020

Accepted Date: 22 May 2020

Please cite this article as: { doi: <https://doi.org/>

This is a PDF file of an article that has undergone enhancements after acceptance, such as the addition of a cover page and metadata, and formatting for readability, but it is not yet the definitive version of record. This version will undergo additional copyediting, typesetting and review before it is published in its final form, but we are providing this version to give early visibility of the article. Please note that, during the production process, errors may be discovered which could affect the content, and all legal disclaimers that apply to the journal pertain.

© 2020 Published by Elsevier.

**Effect of yerba mate extract on the performance of starch films obtained by extrusion and compression molding as active and smart packaging.**

Rocío L. Ceballos<sup>1</sup>, Oswaldo Ochoa-Yepes<sup>1</sup>, Silvia Goyanes<sup>1</sup>, Celina Bernal<sup>2</sup>, Lucía Famá<sup>1\*</sup>.

<sup>1</sup> Universidad de Buenos Aires, Facultad de Ciencias Exactas y Naturales, Departamento de Física, Laboratorio de Polímeros y Materiales Compuestos (LP&MC), Instituto de Física de Buenos Aires (IFIBA-CONICET). Ciudad Universitaria (1428), Ciudad Autónoma de Buenos Aires, Buenos Aires, Argentina.

<sup>2</sup> Instituto de Tecnología en Polímeros y Nanotecnología ITPN, UBA-CONICET, Facultad de Ingeniería, Universidad de Buenos Aires, Av. Las Heras 2214 (1127), Buenos Aires, Argentina.

Rocío Ceballos: rceballos@df.uba.ar

Oswald Ochoa-Yepes: oswaldo@df.uba.ar

Silvia Goyanes: goyanes@df.uba.ar

Celina Bernal: cbernal@fi.uba.ar

\*Dra. Lucía Famá, LPMC, IFIBA-CONICET, Facultad de Ciencias Exactas y Naturales, Universidad de Buenos Aires, Ciudad Universitaria (1428), Pab. 1, Buenos Aires, Argentina. Tel.: +54 11 45763300/9 (ext 255); fax: +54 11 45763357. E-mail address: lfama@df.uba.ar; merfama@hotmail.com.

### Highlights

- Native and hydrolyzed cassava starch/yerba mate extract films were made by extrusion

- Hydrolyzed starch needed less specific energy to gelatinize in the extrusion process
- Film with native starch-10 wt.% of extract was more hydrophobic and tensile resistant
- Hydrolyzed starch with 20 wt.% of extract film showed the highest tensile toughness
- Incorporation of yerba mate extract led to active and smart biodegradable materials

## Abstract

Native or hydrolyzed starch and yerba mate extract (10 wt.% or 20 wt.%) films prepared by extrusion and compression molding were investigated. Native starch material (TPNS) exhibited lower water vapor permeability and higher Young's Modulus ( $E$ ) compared to hydrolyzed starch matrix (TPHS) but decreases in strain at break ( $\epsilon_b$ ) and toughness ( $T$ ). The incorporation of 10 wt.% of extract in TPNS led to greater  $E$  and  $\epsilon_b$  and it resulted the most hydrophobic material. Conversely, TPHS with 20 wt.% of additive resulted the film with the highest  $\epsilon_b$  and  $T$ , indicating a plasticizing effect of the extract in this concentration and system. All materials disintegrated after 10 weeks of burial, contributing to waste reduction. Biofilms containing yerba mate extract showed antioxidant activity and color changes in different pH, indicating their promising role as active and smart packaging for food, in accordance with the new trends for biodegradable and functional packaging.

*Keywords:* Active/smart films; modified starch; yerba mate extract; extrusion/compression molding; physicochemical properties; biodegradability.

## 1. Introduction

Over the last decades, contamination has become a global concern and conventional petroleum-based plastics are an important issue with regards waste management. The food packaging industry is the main plastic demander as it accounts for about half of all used worldwide packaging (de Oliveira & de Melo, 2019), generating high amounts of waste. Due to this problem, the packaging industry has promoted the development of new biodegradable, non-toxic and edible materials. New trends are focused on replacing conventional plastics by biodegradable polymers such as starch, cellulose, alginates and vegetal proteins (Cazón, Velázquez, Ramírez, & Vázquez, 2017; González-Seligra, Eloy-Moura, Famá, Druzian, & Goyanes, 2016; Mishra, Sabu, & Tiwari, 2018; Ochoa-Yepes, Medina-Jaramillo, Guz, & Famá, 2018). Biopolymers based on starch represent an attractive option owing to their low cost, availability and capability of forming thermoplastic films that easily degrade when exposed to specific environmental conditions and bacteria or fungal action (García, Famá, D'Accorso, & Goyanes, 2015; Ghanbarzadeh, Almasi, & Entezami, 2011; Raigond et al., 2019.). However, the biodegradable nature of starch-based materials for packaging was not enough to generate interest among consumers or the industry for commercialization. Therefore, the development of functional materials intended for packaging became attractive to satisfy the needs of modern society.

Functional systems can be categorized into two general groups: active packaging, which actively and deliberately modify the product or the environment it contains during storage, transportation, and even usage to improve the safety and quality of food, and intelligent or smart packaging, which inform the consumer about the kinetic changes related to the quality of the food or the environment it contains, to minimize losses and ensure high quality and safety (Jafarizadeh-Malmiri, Sayyar, Anarjan, & Berenjian, 2019). Intelligent packaging needs to be easy to interpret, quick, reliable, sensitive, safe,

and most importantly cheap, for the visual determination of pH changes, which have been successfully used to evaluate food quality status (Yam, Takhistov, & Miltz, 2005; Yucel, 2016).

In this context, starch-based films result attractive because they can be enriched by the addition of antioxidants, antimicrobials, nutrients and color change indicator components to produce active and intelligent packaging, increasing the shelf life of food (Gutiérrez, González-Seligra, Medina-Jaramillo, Famá, & Goyanes, 2017; Hernández-Muñoz et al., 2019; Silvestre, Duraccio, & Cimmino, 2011). Particularly, the use of antioxidants from natural resources is preferred to avoid synthetic additives, which are associated with negative effects on human health.

Yerba mate (*Ilex paraguariensis*) is a plant rich in polyphenols content, mainly flavonoids and xanthines (Heck & De Mejia, 2007) which has antioxidant, anti-inflammatory and anti-mutagenic properties (Bracesco, Sanchez, Contreras, Menini, & Gugliucci, 2011). The relevant antioxidant and plasticizing effects of yerba mate extract on cassava starch biofilms have been already evaluated in samples obtained by casting (Knapp et al., 2019; Machado, Nunes, Pereira, & Druzian, 2012; Medina-Jaramillo, González-Seligra, Goyanes, Bernal, & Famá, 2015; Medina-Jaramillo, Gutiérrez, Goyanes, Bernal, & Famá, 2016). Additionally, it has been evidenced that anthocyanins (which form part of flavonoids), change their color when exposed to mediums with different pH (Shahid, Islam, & Mohammad, 2013; Veiga-Santos, Ditchfield, & Tadini, 2011).

Nowadays, most research about biodegradable polymers based materials are focused on casting as manufacturing method (Carissimi, Flôres, & Rech, 2018; Feng et al., 2018; Pessanha, Farias, Carvalho, & Godoy, 2018). This is a laboratory scale methodology that implies economical equipment and limited space. However, it allows the production

of small quantities in a long time process, resulting inconvenient for plastic companies, which search for industrial production (large-scale) and without having to invest in new equipment. Consequently, the need to produce with standard equipment used in the manufacture of synthetic polymers triggered the implementation of the extrusion technique to fabricate thermoplastic starch based materials (Guarás, Ludueña, & Álvarez, 2017; Ochoa-Yepes et al., 2018; Pelissari, Yamashita, & Grossmann, 2011). Nevertheless, the extrusion of starch-based materials is much more complex than that of conventional plastics due to the existence of various transitions during processing such as gelatinization, melting, decomposition and recrystallization (Li et al., 2011). Hence, different chemical modifications of starch have been investigated leading to improvements in processability and a decrease in retrogradation of thermoplastic starch-based films (BeMiller, 2018; Dai, Zhang, & Cheng, 2019; Ogunsona, Ojogbo, & Mekonnen, 2018).

A highly relevant chemical process used for the modification of starch, is acid hydrolysis. In a first rapid stage it erodes the amorphous regions of starch granules, breaking  $\alpha$ -D-(1,4) glycosidic linkages then  $\alpha$ -D-(1,6) glycosidic linkages, leading to a polysaccharide with lower molecular weight (Pratiwi, Faridah, & Lioe, 2018). This facilitates the extrusion process, suggesting that hydrolyzed starch could be a feasible alternative to obtain homogeneous films using less process energy.

There is limited research on the effect of acid hydrolysis of starch grains on the properties of thermoplastic films obtained by extrusion and so far, no results are reported in the literature relating the use of this technique together with natural antioxidants to produce active and smart packaging.

The aim of this work was to demonstrate that the use of yerba mate extract in starch-based materials processed by extrusion could generate active and intelligent

biodegradable films of scalable production for its implementation in the food packaging market. In this sense, antioxidant activity, changes in color, as well as morphology, physicochemical properties and biodegradability of films from native and hydrolyzed cassava starch with yerba mate extract obtained by extrusion followed by compression molding were investigated.

## 2. Materials and Methods

### 2.1 Materials

Native cassava starch (with 18 wt.% amylose and 82 wt.% amylopectin, and  $1 \times 10^8$  g/mol molecular weight) and acid hydrolyzed cassava starch ( $1.5 \times 10^5$  g/mol molecular weight) were provided by *Cooperativa Agrícola e Industrial San Alberto Ltda.* (Misiones, Argentina). Yerba mate (*Ilex paraguariensis*) leaves, at the stage of post-drying process and before being subjected to grinding and quality selection, were supplied by *Establecimiento Las Marías* (Corrientes, Argentina). Analytical grade glycerol was purchased from Droquimar S.R.L. (Buenos Aires, Argentina).

### 2.2 Preparation of yerba mate extract

The extract of yerba mate was obtained from infusion following the procedure of Medina-Jaramillo et al. (2015) with modifications and using the quantities suggested by de AR Oliveira, de Oliveira, da Conceição, & Leles (2016).

Yerba mate leaves (100 g) and distilled water (500 mL) were heated at 100 °C for 40 minutes using a magnetic stirrer. The obtained extract was filtered (mesh of ~ 20 µm),

cooled at room temperature ( $\sim 25$  °C) and kept in dark containers under refrigeration (4 °C) until further use. The resultant solids in the extract were around 1.2 g/100 mL (AOAC, 1995).

### *2.3 Films formation*

Films were obtained by extrusion followed by compression molding according to the methodology reported by González-Seligra, Guz, Ochoa-Yepes, Goyanes, & Famá (2017) with some modifications. In a first stage, different systems were prepared by incorporating cassava starch (60 wt.%) to a mixture of glycerol (20 wt.%) and distilled water with the desired yerba mate extract concentration (Table 1), and manually mixing it until complete absorption of the liquid phase into the starch. Afterwards, all mixes were stored 24 h in sealed containers before extrusion (Wang & Ryu, 2013).

To obtain the films, the systems were processed using a co-rotating twin-screw extruder (Nanjing Kerke Extrusion Equipment Co., Ltd., China) with a screw diameter (D) of 16 mm, a length to diameter ratio (L/D) of 40 and a cylindrical die of 4 mm. The screw speed was 80 rpm (with feeding rate of  $\sim 12$  g/min) and the temperature profile was set at 90°C/100°C/110°C/120°C/120°C/130°C/130°C/140°C/130°C/120°C from the feeding zone to the die zone. The threads obtained after extrusion were stabilized during 4 weeks in a conditioned desiccator at 56.7% RH (saturated NaBr) (Famá, Goyanes, & Gerschenson, 2007). Then, films were prepared by compression molding using a hydraulic press with temperature control following the procedure of Gilfillan, Moghaddam, Bartley, & Doherty (2016) with modifications. Pieces of  $\sim 4$  g of the



threads were placed between polytetrafluoroethylene (PTFE) sheets in the press at 120 °C for 15 min at ~ 680 kPa and then 15 min at ~ 3.4 MPa.

The developed films with thickness of  $0.25 \pm 0.05$  mm were stored for 7 days at room temperature in a desiccator at 56.7% RH (saturated NaBr), before being characterized.

## 2.4 Characterizations

Films' characterizations were carried out after 4 weeks of conditioning at 56.7% RH (NaBr) and room temperature.

### 2.4.1 Polyphenols content and antioxidant activity

Total polyphenols content (*TPC*) of the films with yerba mate extract was determined by the Folin–Ciocalteu methodology, following Singleton, Orthofer, & Lamuela-Raventós (1999). To prepare the samples, 400 mg of each film were separately immersed in beakers with 15 mL of distilled water in constant agitation during 24 h at room temperature. Then, 400  $\mu$ L of the dispersion was mixed with 2 mL of Folin–Ciocalteu reagent (1:10 diluted) and 1.6 mL of sodium carbonate (7% w/v). After 30 min dark reaction, absorbance was measured at 760 nm using a spectrophotometer (Shimadzu UV-1800, Japan).

Results were derived from a calibration curve of gallic acid (10-150 mg/L) and expressed in mg gallic acid equivalents (GAE) per gram of film (mg GAE/g). The polyphenols content of the yerba mate extract was studied following the same methodology but using 400  $\mu$ L of the extract to generate the reaction and the results were expressed in mg gallic acid equivalents per gram of extract (mg GAE/g).

The possibility of generating materials for packaging with antioxidant properties can be very useful due to the deleterious role of free radicals in food products. Considering that phenolic compounds are important plant constituents with redox properties, the antioxidant activity of films with yerba mate extract was determined using 1,1-diphenyl-2-picrylhydrazyl (DPPH•) reagent as a free radical, according to the method described by Estevez-Areco, Guz, Famá, Candal, & Goyanes (2019). Films were cut into strips of 500 mg and each sample was immersed in 25 mL of acidic (3% acetic acid v/v), hydrophilic (ethanol 10% v/v) or lipophilic (ethanol 50% v/v) food simulants during 24 h at room temperature in constant agitation at 100 rpm. Then, an aliquot of 100 µL of each simulant was mixed with 3.9 mL of DPPH• in methanol (25 mg/L). After 30 min of reaction, the absorbance was measured at 516 nm using a spectrophotometer (Shimadzu UV-1800) and the percent inhibition (%I) of hydroxyl radical DPPH• was calculated as:

$$\%I = \left( \frac{Abs_w - Abs_s}{Abs_w} \right) \times 100 \quad (1)$$

where  $Abs_w$  is the absorbance of the white (DPPH•) and  $Abs_s$  the absorbance of the sample. Inhibition of DPPH free radicals was compared with a Trolox calibration curve (180–1077 µM), and antioxidant activity was expressed as µM Trolox equivalent per gram of film (µM TE/g).

Similarly, the antioxidant activity of the yerba mate extract was determined using a dilution of the extract in distilled water in a relation 1:250 and results were expressed as (µM TE/g) (Delgado, Galleano, Añón, & Tironi, 2015).

Tests were performed at least 3 times for each sample and the average values were taken.

#### 2.4.2 Fourier transform infrared spectroscopy (FTIR) analysis

Absorbance spectra of yerba mate extract and all films were obtained using a FT/IR-4100 spectrophotometer (Jasco Inc., Japan) with attenuated total reflection (ATR). Spectra were recorded between 4000-400  $\text{cm}^{-1}$  with a resolution of 2  $\text{cm}^{-1}$  and the average of 64 scans were normalized before analysis. The extract was analyzed after being dried in an oven at 110 °C for 20 h, until the complete evaporation of its water content.

Tests were done by triplicate and no-significant differences were observed.

#### *2.4.3 Morphological characterization*

The morphology of the films was evaluated by field emission scanning electron microscopy (FE-SEM, Zeiss Supra 40) of the cryogenic fracture surfaces of the different systems. Samples were cryo-fractured, placed in metal tapes and sputter-coated with platinum (15 s, 0.06 mbar of Ar) before SEM observations.

#### *2.4.4 Susceptibility to water*

##### *2.4.4.1 Moisture content (MC)*

Moisture content of all films (*MC*) was determined through the gravimetric method proposed by the AOAC (1995) with modifications (Morales, Candal, Famá, Goyanes, & Rubiolo, 2015). Pieces of each material (~ 0.5 g) were weighted ( $m_i$ ) and then placed in an oven at 100 °C for 24 h. After that, the samples were weighted again ( $m_f$ ). Moisture content (%) was calculated as:

$$MC = \frac{m_i - m_f}{m_i} \times 100 \quad (2)$$

The results presented are the mean value of 3 sampling units taken from different films.

#### 2.4.4.2 Solubility in water (*S*)

Water solubility values (*S*) for the films were obtained following the method described by Gontard, Duchez, Cuq, & Guilbert (1994) with some modifications. Disks of 2 cm of diameter were placed in an oven at 100 °C for 24 h and then weighted to obtain the initial dry mass ( $m_{si}$ ). Subsequently, these dried disks were immersed in 50 mL of distilled water at 25 °C for 24 h, and after that, they were dried at 100 °C for 24 h to obtain the final dry mass ( $m_{sf}$ ). Water solubility (%) was determined using equation (3):

$$S = \frac{(m_{si} - m_{sf})}{m_{si}} \times 100 \quad (3)$$

The mean value and standard deviation of 3 replicates of each system are reported.

#### 2.4.4.3 Water vapor permeability (*WVP*)

Modified ASTM E96-00 procedure (Famá, Rojo, Bernal, & Goyanes, 2012) was used to measure the water vapor permeability (*WPV*) of all films. Samples were placed into circular acrylic cells with an exposed circular area of  $3.7 \times 10^{-4} \text{ m}^2$ , containing  $\text{CaCl}_2$  as desiccant. Each film sample was sealed over the circular area of the cell and stored at room temperature in desiccators containing NaCl (75% RH). Cells were weighted every 24 h for 7 days, until constant mass. Changes in the weight were plotted as a function of time. *WVP* (g/msPa) was calculated using equation (4):

$$WVP = \frac{G \times e}{A \times S(R_1 - R_2)} \quad (4)$$

Where  $G$ (g/s) is the slope of the plotted curve,  $e$ (m) is the film thickness,  $A$ (m<sup>2</sup>) is the test area,  $S$ (Pa) is the saturation vapor pressure of water at room temperature,  $R_1$  is the relative humidity at the desiccator expressed as a fraction and  $R_2$  is the relative humidity at the acrylic cell expressed as a fraction.

The results shown are the mean value and standard deviation of 3 replicates of each system.

#### 2.4.4.4 Contact angle ( $\theta$ )

Contact angle ( $\theta$ ) measurement is an indicative of the hydrophobicity of polymeric materials. Higher the  $\theta$  value, higher the sample surface hydrophobicity (Pearoval, Debeaufort, Despera, & Voilley, 2002). Contact angle measurements were carried out at room temperature using a Microview USB Digital Microscope coupled with an image analysis software (Analysis Software 220x 2.0 MP) following the methodology described by Guz, Famá, Candal, & Goyanes (2017). A drop of distilled water (2  $\mu$ L) was placed on the surface of each material and immediately photographed. The contact angle was determined as the angle formed by the intersection of the liquid-solid line (drop of water-surface of the film) and the liquid-steam (tangent on the boundary of the drop).

The mean value of 6 measurements are reported.

#### 2.4.5 Mechanical properties

##### 2.4.5.1 Thickness measurement

The thickness value was obtained as a mean of the measurement of at least 10 random positions on the films using a micrometer Micromaster IP54 (TESA-Capasystem) (1  $\mu\text{m}$  resolution).

#### *2.4.5.2 Uniaxial tensile tests*

Uniaxial tensile tests were performed in an Instron dynamometer 5985 at 5 mm/min at room temperature. Samples were cut according to ASTM D882-02 (2002), with 35 mm of effective length and 5 mm of width. Nominal stress( $\sigma$ )-strain( $\varepsilon$ ) curves were recorded and Young's modulus ( $E$ ), tensile strength ( $\sigma_b$ ), strain at break ( $\varepsilon_b$ ), and tensile toughness ( $T$ ) values were obtained from these curves.

At least 10 samples were tested for each system and the average values are reported.

#### *2.4.6 Stability in acidic and alkaline solutions*

The stability and color change of the films in different food simulants (acidic and alkaline solutions) were evaluated in order to determine the possibility of using them as smart packaging. Pieces of each system (16 mm of diameter) were immersed in containers with 10 mL of standard solutions of hydrochloric acid (pH = 3) and sodium hydroxide (pH = 12). The containers were sealed and kept at 25 °C. As it was an accelerated assay, changes in the appearance of the samples immediately 4 min ( $T_1$ ) and 24 h ( $T_2$ ) after immersion were recorded with a Motorola camera of 12 MP.

#### *2.4.7 Biodegradability in vegetable compost*

Biodegradability of all films was qualitatively evaluated at room temperature by disintegration assays according to ISO 20200 (2015). Samples of each system (20 mm × 20 mm) were weighed and then buried in plastic trays of 10 × 20 × 5 cm (length × length × height) filled with vegetable compost (soil), ensuring that the samples were at a depth of around 1 cm. The humidity of soil was controlled by spraying with water once a day. Samples were carefully taken out once a week and photographed.

#### *2.4.8 Data processing and statistical analysis*

Data analysis was carried out using two-way ANOVA with 95% confidence level ( $p < 0.05$ ) and Tukey post-hoc test. The results are reported as the mean and standard deviation, and for comparison “T” test was applied.

### **3. Results and discussion**

#### *3.1. Total polyphenols content and antioxidant activity*

Table 2 shows the total polyphenols content of the developed films. Considering that the total polyphenols content of the yerba mate extract was  $(17 \pm 1)$  mg GAE/g, it should be noted that the films retained the 100% of the polyphenols contained in the extract before being processed. In addition, for both types of starch, the polyphenols content increases with the extract content, as was expected. When the extract content in TPNS-Y20 and TPHS-Y20 was twice that of TPNS-Y10 and TPHS-Y10, respectively,

the polyphenols content was duplicated. No significant differences between the results of TPNS and TPHS for 10 wt.%, neither for 20 wt.% of extract were observed.

The antioxidant activity of the developed films in different media is also shown in table 2. Biofilms with higher content of yerba mate extract showed higher antioxidant activity in all food simulants. For TPNS-Y20 and TPHS-Y20 it was nearly twice that of TPNS-Y10 and TPHS-Y10, respectively. Significant differences in the antioxidant activity of the same material in different simulants were found, indicating that the polyphenols activity depends on the medium. For every developed film, the higher antioxidant activity was observed in lipophilic medium. According to the literature, this behavior is possibly due to the presence of lipophilic components of the yerba mate extract such as tocopherols (Souza et al., 2015).

### *3.2 Fourier transform infrared spectroscopy (FTIR) analysis*

Fig. 1 shows main normalized ATR-FTIR spectra of dried yerba mate extract and the different developed films. Fig. 1B is the magnification of Fig. 1A in the region from  $900\text{ cm}^{-1}$  to  $1100\text{ cm}^{-1}$ . As regards the extract, the broad band observed in the region from  $3600\text{ cm}^{-1}$  to  $3000\text{ cm}^{-1}$  can be associated to the vibration of OH and acid and alcohols groups present in Chlorogenic acid, Saponins, and primary amines of Theobromine and Caffeine that are contained in the extract (Medina-Jaramillo et al., 2015; Silverstein, Webster, Kiemle, & Bryce, 2014). The absorption peak at around  $2922\text{ cm}^{-1}$  is due to a stretching vibration of aliphatic CH, and the bands observed between  $1800\text{ cm}^{-1}$  and  $1500\text{ cm}^{-1}$  correspond to the carbonyl group of esters, amides, acids and other compounds such as Xanthines and Saponins, existing in yerba mate



(Marcelo, Pozebon, & Ferrão, 2015). The bands in the regions between  $1500\text{ cm}^{-1}$  and  $1000\text{ cm}^{-1}$  are related to the stretching vibration of the C-O (Schneider et al., 2018).

Films exhibited the typical behavior of thermoplastic starch based materials (Pereira Jr, de Arruda, & Stefani, 2015; Warren, Gidley, & Flanagan, 2016). They showed the significant absorption peak at  $3600\text{-}3000\text{ cm}^{-1}$  corresponding to O-H stretching, a double peak at  $3000\text{-}2800\text{ cm}^{-1}$  associated to C-H stretching, bands at  $1150\text{-}1100\text{ cm}^{-1}$  (C-O, C-C and C-O-H stretching), a double peak at  $1100\text{-}990\text{ cm}^{-1}$  (C-O-H bending), and the bands at  $\sim 930\text{ cm}^{-1}$ ,  $860\text{ cm}^{-1}$  and  $760\text{ cm}^{-1}$  (vibrations of glycosidic ring).

It is noted that the intensity of the band around  $3300\text{ cm}^{-1}$  resulted slightly higher in TPHS compared to TPNS. This peak is strongly related to available and not-available OH groups (Grace & Liew, 2016) thus, the higher intensity may indicate the presence of more OH groups in the hydrolyzed starch matrix. This behavior is a consequence of the hydrolysis process that breaks the starch chains leading to a larger number of the extreme of chains with OH (González-Seligra et al., 2016). Chemical modification of starch did not significantly modify the other mentioned peaks.

The films prepared with native starch and yerba mate extract (TPNS-Y10 and TPNS-Y20) presented slightly higher intensity in the peak at  $\sim 3300\text{ cm}^{-1}$  with respect to TPNS, that can be due to components present in yerba mate such as Chlorogenic acid, Saponins, Theobromine and Caffeine (Silverstein et al., 2014), and/or OH groups of the extract, which contribute to the amount of OH in those films. In the case of the materials prepared with hydrolyzed starch and yerba mate extract (TPHS-Y10 and TPHS-Y20), no significant differences with respect to TPHS were observed at this band. No significant changes were observed in the band at around  $1638\text{ cm}^{-1}$  related to the stretching and bending vibration of hydrogen bonding O-H groups of the water

(Minakawa, Faria-Tischer, & Mali, 2019; Qin, Liu, Jiang, Xiong, & Sun, 2016), contrary to the observations of Medina-Jaramillo et al. (2015) in starch-extract films prepared by casting. This is expectable taking into account that casting involves higher amount of water than extrusion. During extrusion, the interactions between starch-glycerol and yerba mate extract were not enough to alter infrared spectra. The effect of yerba mate extract incorporation was observed in the range from  $1050\text{ cm}^{-1}$  to  $1020\text{ cm}^{-1}$ , as there was an increase in peak intensity around  $1022\text{ cm}^{-1}$  in the films containing the extract (Fig. 1B). The band at about  $1040\text{ cm}^{-1}$  of yerba mate extract curve, which is related to polyphenols (García et al., 2019), seemed to overlap with that corresponding to C-O-H vibrations of starch (at  $\sim 1022\text{ cm}^{-1}$ ), according to the observations of Estevez-Areco et al. (2019) in starch-rosemary extract films. This behavior can be attributed to the presence of yerba mate extract polyphenols.

### *3.3 Morphological analysis by SEM*

Cryogenic fracture surface micrographs (FE-SEM) of the films are presented in Fig. 2.

The native starch film (TPNS) exhibited a smooth surface without holes or cracks but with not well-dispersed broken starch grains of micrometric size (smaller than  $2\text{ }\mu\text{m}$ ), which seemed to be not-agglomerated (Fig. 2a). Different authors observed partly melted starch granules in extruded films, concluding that incomplete starch gelatinization occurred after extrusion and compression molding processes. These results indicate that the shear strength necessary to gelatinize the starch was insufficient (Pushpadass, Marx, Wehling, & Hanna, 2008).

The film with hydrolyzed starch (TPHS) also presented a smooth surface without holes but with lower density of broken starch granules than the TPNS film (Fig. 2b), suggesting that the chemical modification led to better starch gelatinization during extrusion and indicating that less specific mechanical and thermal energy was necessary to gelatinize the starch. This behavior can be attributed to the short chains of the hydrolyzed starch (lower molecular weight) that make it easier to process as they generate a more open network, so the diffusion of water molecules is faster, facilitating gelatinization (González-Seligra et al., 2016).

The incorporation of yerba mate extract on native starch films contributed to the starch gelatinization. In particular, in the case of the film with 10 wt.% of the extract (TPNS-Y10), a smooth surface without holes and with only few broken starch granules smaller than 1  $\mu\text{m}$  was observed (Fig. 2c). This material also showed oriented lines that may indicate a strong interaction possibly between the additive and the starch (Ochoa-Yepes, Di Giorgio, Goyanes, Mauri, & Famá, 2019).

When 20 wt.% of the extract was incorporated (TPNS-Y20), a rough cryo-fractured surface was observed without broken starch grains or holes (Fig. 2e). This type of surface is typical of a plasticized material (García, Ribba, Dufresne, Aranguren, & Goyanes, 2011). All the evaluated films were made with the same amount of plasticizer and therefore, the change in the material's morphology would suggest that the extract incorporated in larger concentrations in the native starch matrix would be acting as a plasticizer (Medina-Jaramillo et al., 2015). In addition, oriented lines were observed, which may indicate that the increment in the amount of extract led to more interactions. Therefore, the addition of yerba mate extract to native starch favors its gelatinization by reducing the mechanical and thermal energy required during extrusion.

The effect of yerba mate extract on hydrolyzed starch films did not eliminate broken starch grains as they still appeared in TPHS-Y10 (Fig. 2d) and, although in a lesser extent, in TPHS-Y20 (Fig. 2f).

### 3.3 Susceptibility to water

Results of the susceptibility to water assays performed on the different films are reported in Table 3.

Moisture content of TPNS was in accordance with the values reported in the literature for starch films made by extrusion (Gutiérrez, Toro-Márquez, Merino, & Mendieta, 2018; Ochoa-Yepes et al., 2019), while solubility resulted higher and *WVP* lower than those reported by other authors (González-Seligra et al., 2017). Considering that water vapor permeability of a film in the packaging industry is related to its capability to control the water vapor transmission (WVT) between a product and the environment, a lower value of *WVP* is advantageous as it implies a limitation on WVT, preserving the shelf life of the product. It is well known that permeability depends on the solubility and diffusivity of water in the polymeric matrix. A decrease in *WVP* value of TPNS with respect to those reported in the literature could be due to the interruption in the diffusion path created by the broken starch grains distributed in the polymeric matrix observed in SEM micrographs (Fig. 2a). The tortuous path formed is capable of reducing the diffusion rate of molecules through the film, leading to a decrease of water permeability (Slavutsky, Bertuzzi, Armada, García, & Ochoa, 2014).

Hydrolyzed starch matrix exhibited increases in all the susceptibility to water values compared to those of TPNS. The increment in  $S$  is consistent to observations made by other authors who related this behavior with the hydrolysis process (Luchese, Frick, Patzer, Spada, & Tessaro, 2015; Wang & Copeland, 2015; Wang, Thruong, & Wang, 2003). As reported in the literature, higher values of  $MC$  in TPHS could be due to the hydrolysis process, which breaks the starch chains, generating additional extremes of chains and therefore producing a more open packing and more free OH that facilitates the absorption of water (González-Seligra et al., 2016). The increase in  $WVP$  can be attributed to this fact and to the slightly lower number of broken grains in TPHS compared to TPNS detected in SEM micrographs. Furthermore, susceptibility to water behavior of TPHS is consistent to the lower value of the contact angle with respect to that of TPNS (Fig. 3), indicating that the chemical modification hydrophilized the modified films surface.

The incorporation of 10 wt.% yerba mate extract in native starch films (TPNS-Y10) led to an increasing trend of  $MC$  and  $S$  values but without significant differences. However, there was a slight decrease of  $WVP$  in near 15%. This could be attributed to the fact that although there are almost no broken grains in TPNS-Y10, which would lead to an increase in permeability, the great interaction between the extract and the starch suggested by SEM analysis, could have made water molecules move through a tortuous path when diffused across the polymer matrix (Slavutsky et al., 2014), leading to a decrease in  $WVP$ . In native starch films containing 20 wt.% (TPNS-Y20) no significant differences in  $MC$  and  $S$  values were detected but a slight increasing trend of the  $MC$  value was observed, while  $WVP$  value increased in almost 47%. SEM analysis for this material revealed a different morphology with respect to TPNS and TPNS-Y10 and similar to a highly plasticized starch-based material. According to the literature, an

increment in the content of the plasticizer in starch films leads to an increase in *WVP* (Chillo et al., 2008; Guo et al., 2012; Pushpadass et al., 2008). Therefore, yerba mate extract in the highest concentration incorporated into cassava native starch matrix could be acting as a plasticizer, as it was reported by Reis et al. (2015).

For modified starch films, no significant differences were found in both *MC* and water solubility, while *WVP* slightly increased with the incorporation of yerba mate extract, as it resulted higher in almost 28% in TPNS-Y10 and 10% in TPNS-Y20.

Although the presence of broken grains in these materials may cause a tortuous path for the water molecules and therefore diminish *WVP*, the increment in the values of *WVP* could be explained by the plasticizing effect of the extract. As the same amount incorporated in other samples is now distributed in the region without grains, the concentration of extract is higher there and may act as plasticizer.

In order to evaluate the effect of both the starch modification and the extract incorporation in the hydrophilicity of the films, the contact angle ( $\theta$ ) between a drop of water and the surface of a film (angle of deposition) was measured (Fig. 3). It is well known that wettability is strongly influenced by the contact angle and it is greatly related to the hydrophobicity of the film (Abreu et al., 2015; Vogler, 1998). Higher  $\theta$  indicates less hydrophilicity.

Although the contact angle values for native starch film ( $60 \pm 5^\circ$ ) and for modified starch sample ( $56 \pm 4^\circ$ ) did not present significant differences, an increasing trend of the values for TPNS compared to those for TPNS was observed, indicating more hydrophobicity in the native starch film. This is consistent with susceptibility to water behavior, as it presented slightly lower values of *MC* and water solubility than TPNS. The presence of less availability OH groups leads to a lower affinity to the aqueous medium, then to a more hydrophobic material (Ochoa-Yepes et al., 2019).

For native starch films, the incorporation of 10 wt.% of yerba mate extract did not change significantly the contact angle with respect to TPNS, being  $62 \pm 4^\circ$ , while the addition of 20 wt.% of the extract provoked a decrease in  $\theta$  of almost 40%, indicating a more hydrophilic surface for TPNS-Y20. This behavior accords with the hypothesis that the extract can act as a plasticizer when incorporated in this concentration in the native starch matrix. In the case of films processed with hydrolyzed starch, the incorporation of both concentrations of yerba mate extract led to a decrease of the values of  $\theta$ , indicating higher hydrophilicity with respect to TPHS, and being consistent with *WVP* values (Table 3). Particularly, the lowest value of  $\theta$  corresponds to TPHS-Y20, probably due to the effect of the extract acting as plasticizer, being a consequence of the higher concentration in the zones without broken grains in the sample.

### 3.4 Mechanical behavior

Tensile parameters values for all systems investigated are presented in Table 4. Films obtained from native starch (TPNS) presented higher modulus and stress at break values but lower strain at break values than similarly prepared thermoplastic starch films reported in the literature (González-Seligra et al., 2017; Ochoa-Yepes et al., 2019). This behavior could be attributed to the presence of broken starch grains as it was observed in SEM micrographs (Fig. 2a). On the one hand, starch grains have a rigid structure and could act as reinforcement (Li et al., 2011), contributing to the material mechanical strength (Gutiérrez, Tapia, Pérez, & Famá, 2015; Sun, Liu, Ji, Hou, & Dong, 2017). On the other hand, the presence of grains could lead to a material with smaller strain at break as a result of premature failure.

Modified starch films showed a decrease in the  $E$  value and presented higher  $\varepsilon_b$  value than TPNS, indicating more flexibility. TPHS have less broken grains than TPNS and also slightly more water content. Although the mechanical behavior could be affected by both factors, the difference in morphology has probably a higher effect than the change in humidity which is also very slight. Furthermore, strain at break in TPHS resulted higher because the probability of cracks is smaller as there are less broken grains. Tensile toughness for TPHS is higher than TPNS, due to the increase in the strain at break. Therefore, the use of the hydrolyzed starch led to a more flexible material with also higher tensile toughness.

The effect of the incorporation of yerba mate extract was different, depending on the amount introduced and the type of starch. For TPNS-Y10, both  $E$  and  $\varepsilon_b$  presented a slight trend to increase compared to TPNS, as expectable considering the trends observed in WC and hydrophobicity behavior of those films, as well as the decrease in the number of broken starch grains and therefore in the probability of cracks.

Additionally, morphological analysis indicates the presence of a great interaction between starch and the extract, which leads to increments in those parameters. In TPNS-Y20, a decrease in  $E$  and an increase in  $\varepsilon_b$  are clearly observed, confirming the plasticizing effect of the extract. These results are consistent with the morphology observed in the SEM micrographs. In both cases, tensile toughness was higher than in TPNS. In TPNS-Y10, this was a result of the increase in  $E$  and  $\varepsilon_b$ , while in TPNS-Y20 depended on the increase in  $\varepsilon_b$ , as it was more relevant than the decrease in  $E$ .

The incorporation of yerba mate extract in modified starch films caused an increment in  $E$  without significant changes in  $\sigma_b$ , regardless of the concentration used. Considering that SEM micrographs showed in TPHS-Y10 and TPHS-Y20 broken grains as in TPHS,



higher values of  $E$  could be attributed to a good interaction between the extract and starch. Since hydrolysis acidic modification led to a starch with a higher number of short chains, it can be expected that more interactions occur between the extract and modified starch than with the native starch. Strain at break for TPHS-Y10 and TPHS showed no significant differences, whereas  $\sigma_b$  of TPHS-Y20 increased in nearly 15%, possibly due to the great interaction between the extract and matrix components and the effect of the yerba mate extract, already observed by other authors, which led to improvements in flexibility (Knapp et al., 2019). Tensile toughness in TPHS-Y10 presents no significant differences with TPHS while in TPHS-Y20, it increased in 33% with respect to TPHS, due to the significant increase in  $\varepsilon_b$ .

Higher  $T$  values are remarkable as tensile toughness is one of the key mechanical properties of bio-based packaging films, and mechanical integrity is important for protection and tampering resistance of food packaging, ensuring safety and high quality of the products for the consumer (Briassoulis & Giannoulis, 2018).

### *3.5 Stability in acidic or alkaline solutions*

Since food packaging industries produce coatings for products with a wide range of pH (such as meat, cheese and fruits), it is essential to evaluate films' stability and color change in different food simulants (acidic and alkaline solutions) to determine whether they could be used as smart packaging.

Images of the different films in air and after immersion in an acidic or alkaline medium are presented in Fig. 4. As it was an accelerated assay, the response to different pH was photographed 4 min and 24 h after being immersed ( $T_1$  and  $T_2$ , respectively).

Initially, all samples had a diameter of ~ 16 mm and presented slight increments of diameter after being immersed in the solutions.

In native starch based films at  $T_1$ , the broadening was between 15-25% in acidic or alkaline media. For hydrolyzed starch samples, the increase resulted of around 30% in acidic solution. In alkaline medium, TPHS widened about 40%, while TPHS-Y10 and TPHS-Y20 around 30% and 25%, respectively, indicating that the extract limited the swelling of hydrolyzed starch films in those media. It is notorious that all films remained unbroken at  $T_1$ .

After 24 hours ( $T_2$ ) in acidic medium, samples were practically not widened with respect to  $T_1$  (no significant changes in diameter were observed) and were whole, showing stability at pH = 3 until the end of the measurements. This behavior is very important considering the possible use of the films in contact with acidic foods like most of fruits and meats in the market. In alkaline medium, the samples prepared with native starch, independently of the addition of the extract, began to disintegrate, while the films based on hydrolyzed starch remained whole.

With respect to the films' color, all systems exhibited a slightly whiter color during the test in the acidic solution. After being immersed in the alkaline medium, films without yerba mate extract did not show any change in color, while films containing extract notoriously did, as it can be seen at  $T_1$ . All samples exhibited a yellow-orange-brown tone at  $T_1$ , although for TPHS-Y10 and TPHS-Y20 it was lighter. According to the literature, the change in the color of the samples with the extract could be attributed to the anthocyanins (Shahid et al., 2013; Veiga-Santos et al., 2011) derived from cyanidin components of yerba mate (Ricco, Wagner, Giberti, & Gurni, 1995). Color changes in the films containing yerba mate extract when the pH varies are relevant since these

systems could be used as food coatings, indicating the pH and therefore the quality of coated food, similarly as an intelligent packaging (Yoshida, Maciel, Mendonça, & Franco, 2014). During storage, several food products suffer changes in pH due to their normal metabolic processes or as a consequence of bacterial contamination (Ma, Du, & Wang, 2017). For example, the growth in the population of *Pseudomonas* in chicken breast fillets investigated by Wang et al. (2017) led to an increase in pH value.

Furthermore, an increase in pH due to the endogenous and microbial enzymes produced during the storage of meat products was reported (Barrientos, Chabela, Montejano, & Guerrero Legarreta, 2006).

Finally, after 24 hours ( $T_2$ ), the four systems containing the extract almost returned to their original tone, leaving a different color in the solution, thus indicating the total extract release in this medium.

### *3.6 Biodegradability in vegetal compost*

The macroscopic appearance of the films as a function of the time of burial in vegetable compost was analyzed from the photographs shown in Figure 5. Weight values for the films could not be accurately obtained as residual soil affected weight measurements.

After 2 weeks of burial, all systems presented changes in their tonality. Films made from modified starch exhibited holes and more marked breakdowns than those based on native starch. After 4 weeks, native starch films started exhibiting breakdowns more evidently while TPHS, TPHS-Y10 and TPHS-Y20 already showed much more breakage, indicating that they had degraded faster than samples made from native starch. This behavior is clearly observed from the images taken after 8 weeks of burial,

when the films containing the hydrolyzed starch were almost completely degraded as TPNS, TPNS-Y10 and TPNS-Y20 did so only after 10 weeks.

The faster biodegradability of hydrolyzed starch based films is consistent with the results of water solubility and hydrophobicity of these samples. Water solubility is a determining factor for the biodegradability of films (Raigond et al., 2019) and higher water solubility leads to faster biodegradation. On the other hand, the lower molecular weight of hydrolyzed starch could lead to earlier degradation in compost. It is known that microorganisms break down starch chains into smaller units of sugars that are eventually converted to glucose, which is the individual basic unit (Azahari, Othman, & Ismail, 2011). For a lower molecular weight starch (with shorter chains), this process occurs in less time, thus the faster biodegradability of hydrolyzed starch materials was expectable.

Results from biodegradability assays indicated that for both types of starch, there was no contrast between films with and without yerba mate extract. The main differences between films were attributed to the type of starch. Finally, all films demonstrated to be biodegradable in vegetable compost, being degraded almost completely after ten weeks. This phenomenon, which occurs in the materials based on starch prepared by extrusion and subsequent compression molding, and persists with the incorporation of the natural extract of yerba mate, generates a great attraction for their implementation towards cleaner alternatives.

#### **4. Conclusions**

Films of native or hydrolyzed starch containing two concentrations of yerba mate extract (10 wt.% and 20 wt.%) were developed. Native starch matrix exhibited a smooth

surface without holes or cracks but with not well-dispersed broken starch grains, while TPHS presented a lower density of broken starch granules, suggesting that the chemical modification led to better starch gelatinization during extrusion and indicating that less specific mechanical and thermal energy were necessary to gelatinize the starch. TPNS showed decreases in water solubility, moisture content and water vapor permeability values compared with those of hydrolyzed starch TPHS and it resulted hydrophobic. In addition, the matrix from native starch presented higher modulus and stress at break values than TPHS and those reported in the literature, while modified starch sample showed lower  $E$  and higher  $\varepsilon_b$ , indicating more flexibility. The incorporation of yerba mate extract led to active and smart biodegradable materials. The extract polyphenols remained in the starch films and were then released in different media, showing them as active materials. In addition, yerba mate extract led to changes in the color of the films when exposed to different pH media, leading to intelligent materials. The extract incorporation of 10 wt.% in native starch films was evidenced by a reduction in the density of broken starch granules and the appearance of oriented lines, indicating a strong interaction possibly between the additive and the starch. These films resulted the most hydrophobic material and showed a decrease in  $WVP$  and a trend to increase in both  $E$  and  $\varepsilon_b$ . When 20 wt.% of yerba mate extract was added (TPNS-Y20), a rough cryo-fractured surface typical of a plasticized material was observed. As expectable, a decrease in  $E$  and an increase in  $\varepsilon_b$  were observed, confirming the plasticizing effect of the extract. TPNS-Y20 resulted the most hydrophilic material. The incorporation of yerba mate extract in hydrolyzed starch films caused a slight increase in  $WVP$  and in  $E$ , without significant changes in  $\sigma_b$ , regardless of the concentration used. Tensile toughness only showed significant differences compared to TPHS when 20 wt.% of the extract was incorporated (TPHS-Y20), as it increased in a 33%. Results from

biodegradability assays revealed that after 10 weeks of burial, all films were disintegrated, showing no contrast between films with and without yerba mate extract. This investigation showed that biofilms developed with yerba mate extract are promising active and smart materials to replace the use of conventional plastic in food packaging, not only to reduce waste but also to improve the shelf life of food.

### **Credit Author Statement**

Drs. Lucía Famá and Celina Bernal conceived of the presented idea. They developed the theory, performed the experiments to carry out and supervised the project.

Rocío Ceballos carried out the experiment and wrote the manuscript with support from Oswaldo Ochoa-Yepes.

Dr. Silvia Goyanes helped supervise the project.

All authors discussed the results and contributed to the final manuscript.

Declarations of interest: none

### **Acknowledgements**

The authors would like to thank *Cooperativa Agrícola e Industrial San Alberto Limitada* (C.A.I.S.A., Costa Rica, Misiones, Argentina) for the starches donation.

Funding: This work was supported by Agencia Nacional de Promoción científica y Tecnológica (ANPCyT PICT 2017-2362 and PICT Startup 2016-4639), Secretaría de Política Universitarias (SPU N° 1655), Universidad de Buenos Aires (UBACyT 2018 20020170100381BA y UBACyT 2018 20020130100696BA),

## References

- Abreu, A. S., Oliveira, M., de Sá, A., Rodrigues, R. M., Cerqueira, M. A., Vicente, A. A., & Machado, A. V. (2015). Antimicrobial nanostructured starch based films for packaging. *Carbohydrate polymers*, *129*, 127-134.
- AOAC, (1995). Official methods of analysis. *Washington, DC: Association of Official Analytical Chemists*.
- ASTM, E. D882-02 (2002). *Standard Test Method for Tensile Properties of Thin Plastic Sheeting in manual book of ASTM standards, American Society for Testing and Materials*.
- Azahari, N. A., Othman, N., & Ismail, H. (2011). Biodegradation studies of polyvinyl alcohol/corn starch blend films in solid and solution media. *Journal of Physical Science*, *22*(2), 15-31.
- Barrientos, R. G., Chabela, M. P., Montejano, J. G., & Legarreta, I. G. (2006). Changes in pork and shark (*Rhizopriondon terraenovae*) protein emulsions due to exogenous and endogenous proteolytic activity. *Food research international*, *39*(9), 1012-1022.
- BeMiller, J. N. (2018). *Carbohydrate chemistry for food scientists*. Elsevier.
- Bracesco, N., Sanchez, A. G., Contreras, V., Menini, T., & Gugliucci, A. (2011). Recent advances on *Ilex paraguariensis* research: minireview. *Journal of ethnopharmacology*, *136*(3), 378-384.
- Briassoulis, D., & Giannoulis, A. (2018). Evaluation of the functionality of bio-based food packaging films. *Polymer Testing*, *69*, 39-51.
- Carissimi, M., Flôres, S. H., & Rech, R. (2018). Effect of microalgae addition on active biodegradable starch film. *Algal research*, *32*, 201-209.

- Cazón, P., Velazquez, G., Ramírez, J. A., & Vázquez, M. (2017). Polysaccharide-based films and coatings for food packaging: A review. *Food Hydrocolloids*, 68, 136-148.
- Chillo, S., Flores, S., Mastromatteo, M., Conte, A., Gerschenson, L., & Del Nobile, M. A. (2008). Influence of glycerol and chitosan on tapioca starch-based edible film properties. *Journal of Food Engineering*, 88(2), 159-168.
- Dai, L., Zhang, J., & Cheng, F. (2019). Effects of starches from different botanical sources and modification methods on physicochemical properties of starch-based edible films. *International Journal of Biological Macromolecules*, 132, 897-905.
- de AR Oliveira, G., de Oliveira, A. E., da Conceição, E. C., & Leles, M. I. (2016). Multiresponse optimization of an extraction procedure of carnosol and rosmarinic and carnosic acids from rosemary. *Food chemistry*, 211, 465-473.
- de Oliveira, A. S. B., & de Melo, N. R. (2019). MARKET AND SUSTAINABILITY OF FOOD PACKAGING: A REVIEW. *Boletim do Centro de Pesquisa de Processamento de Alimentos*, 36(1).
- Delgado, M. C. O., Galleano, M., Añón, M. C., & Tironi, V. A. (2015). Amaranth peptides from simulated gastrointestinal digestion: antioxidant activity against reactive species. *Plant foods for human nutrition*, 70(1), 27-34.
- Estevez-Areco, S., Guz, L., Famá, L., Candal, R., & Goyanes, S. (2019). Bioactive starch nanocomposite films with antioxidant activity and enhanced mechanical properties obtained by extrusion followed by compression molding. *Food Hydrocolloids*, 96, 518-528.
- Famá, L., Goyanes, S., & Gerschenson, L. (2007). Influence of storage time at room temperature on the physicochemical properties of cassava starch films. *Carbohydrate Polymers*, 70(3), 265-273.



Famá, L., Rojo, P. G., Bernal, C., & Goyanes, S. (2012). Biodegradable starch based nanocomposites with low water vapor permeability and high storage modulus.

*Carbohydrate Polymers*, 87(3), 1989-1993.

Feng, M., Yu, L., Zhu, P., Zhou, X., Liu, H., Yang, Y., ... & Chen, P. (2018).

Development and preparation of active starch films carrying tea polyphenol. *Carbohydrate polymers*, 196, 162-167.

García, N. L., Famá, L., D'Accorso, N. B., & Goyanes, S. (2015). Biodegradable starch nanocomposites. In *Eco-friendly polymer nanocomposites* (pp. 17-77). Springer, New Delhi.

García, N. L., Ribba, L., Dufresne, A., Aranguren, M., & Goyanes, S. (2011). Effect of glycerol on the morphology of nanocomposites made from thermoplastic starch and starch nanocrystals. *Carbohydrate polymers*, 84(1), 203-210.

García, F. E., Senn, A. M., Meichtry, J. M., Scott, T. B., Pullin, H., Leyva, A. G., ..., & Requejo, F. G. (2019). Iron-based nanoparticles prepared from yerba mate extract. Synthesis, characterization and use on chromium removal. *Journal of environmental management*, 235, 1-8.

Ghanbarzadeh, B., Almasi, H., & Entezami, A. A. (2011). Improving the barrier and mechanical properties of corn starch-based edible films: Effect of citric acid and carboxymethyl cellulose. *Industrial Crops and products*, 33(1), 229-235.

Gilfillan, W. N., Moghaddam, L., Bartley, J., & Doherty, W. O. (2016). Thermal extrusion of starch film with alcohol. *Journal of Food Engineering*, 170, 92-99.

Gontard, N., Duchez, C., CUQ, J. L., & Guilbert, S. (1994). Edible composite films of wheat gluten and lipids: water vapour permeability and other physical properties.

*International journal of food science & technology*, 29(1), 39-50.

- Gonzalez-Selgra, P., Eloy Moura, L., Famá, L., Druzian, J. I., & Goyanes, S. (2016). Influence of incorporation of starch nanoparticles in PBAT/TPS composite films. *Polymer International*, 65(8), 938-945.
- González-Selgra, P., Guz, L., Ochoa-Yepes, O., Goyanes, S., & Famá, L. (2017). Influence of extrusion process conditions on starch film morphology. *LWT*, 84, 520-528.
- Grace, S., & Liew, K. C. (2016). Hydrolyzation of Edible Starches: Their Preparations and Properties. *In Materials Science Forum* (Vol. 875, pp. 63-76). Trans Tech Publications.
- Guo, X., Lu, Y., Cui, H., Jia, X., Bai, H., & Ma, Y. (2012). Factors affecting the physical properties of edible composite film prepared from zein and wheat gluten. *Molecules*, 17(4), 3794-3804.
- Gutiérrez, T. J., Seligra, P. G., Jaramillo, C. M., Famá, L., & Goyanes, S. (2017). Effect of filler properties on the antioxidant response of thermoplastic starch composites. *In Handbook of composites from renewable materials, structure and chemistry* (Vol. 1, pp. 337-370). John Wiley & Sons.
- Gutiérrez, T. J., Tapia, M. S., Pérez, E., & Famá, L. (2015). Structural and mechanical properties of edible films made from native and modified cush-cush yam and cassava starch. *Food Hydrocolloids*, 45, 211-217.
- Gutiérrez, T. J., Toro-Márquez, L. A., Merino, D., & Mendieta, J. R. (2019). Hydrogen-bonding interactions and compostability of bionanocomposite films prepared from corn starch and nano-fillers with and without added Jamaica flower extract. *Food Hydrocolloids*, 89, 283-293.

- Guz, L., Famá, L., Candal, R., & Goyanes, S. (2017). Size effect of ZnO nanorods on physicochemical properties of plasticized starch composites. *Carbohydrate polymers*, 157, 1611-1619.
- Heck, C. I., & De Mejia, E. G. (2007). Yerba Mate Tea (*Ilex paraguariensis*): a comprehensive review on chemistry, health implications, and technological considerations. *Journal of food science*, 72(9), R138-R151.
- Hernández-Muñoz, P., Cerisuelo, J. P., Domínguez, I., López-Carballo, G., Catalá, R., & Gavara, R. (2019). *Nanotechnology in Food Packaging*. In *Nanomaterials for Food Applications* (pp. 205-232). Elsevier.
- International Organization for Standardization (2015). Determination of the degree of disintegration of plastic materials under simulated composting conditions in a laboratory-scale test (ISO Standard No.20200:2015). Retrieved from <https://www.iso.org/standard/63367.html>
- Jafarizadeh-Malmiri, H., Sayyar, Z., Anarjan, N., & Berenjian, A. (2019). Nanobiotechnology in Food Packaging. In *Nanobiotechnology in Food: Concepts, Applications and Perspectives* (pp. 69-79). Springer, Cham.
- Knapp, M. A., dos Santos, D. F., Pilatti- Riccio, D., Deon, V. G., dos Santos, G. H. F., & Pinto, V. Z. (2019). Yerba mate extract in active starch films: Mechanical and antioxidant properties. *Journal of Food Processing and Preservation*, e13897.
- Li, M., Liu, P., Zou, W., Yu, L., Xie, F., Pu, H., ..., & Chen, L. (2011). Extrusion processing and characterization of edible starch films with different amylose contents. *Journal of Food Engineering*, 106(1), 95-101.
- Luchese, C. L., Frick, J. M., Patzer, V. L., Spada, J. C., & Tessaro, I. C. (2015). Synthesis and characterization of biofilms using native and modified pinhão starch. *Food hydrocolloids*, 45, 203-210.

- Ma, Q., Du, L., & Wang, L. (2017). Tara gum/polyvinyl alcohol-based colorimetric NH<sub>3</sub> indicator films incorporating curcumin for intelligent packaging. *Sensors and Actuators B: Chemical*, 244, 759-766.
- Machado, B. A. S., Nunes, I. L., Pereira, F. V., & Druzian, J. I. (2012). Desenvolvimento e avaliação da eficácia de filmes biodegradáveis de amido de mandioca com nanocelulose como reforço e com extrato de erva-mate como aditivo antioxidante. *Ciência Rural*, 42(11), 2085-2091.
- Marcelo, M. C., Pozebon, D., & Ferrão, M. F. (2015). Authentication of yerba mate according to the country of origin by using Fourier transform infrared (FTIR) associated with chemometrics. *Food Additives & Contaminants: Part A*, 32(8), 1215-1222.
- Medina-Jaramillo, C., González Seligra, P., Goyanes, S., Bernal, C., & Famá, L. (2015). Biofilms based on cassava starch containing extract of yerba mate as antioxidant and plasticizer. *Starch - Stärke*, 67(9-10), 780-789.
- Medina-Jaramillo, C., Gutiérrez, T. J., Goyanes, S., Bernal, C., & Famá, L. (2016). Biodegradability and plasticizing effect of yerba mate extract on cassava starch edible films. *Carbohydrate Polymers*, 151, 150-159.
- Minakawa, A. F., Faria-Tischer, P. C., & Mali, S. (2019). Simple ultrasound method to obtain starch micro-and nanoparticles from cassava, corn and yam starches. *Food chemistry*, 283, 11-18.
- Mishra, R. K., Sabu, A., & Tiwari, S. K. (2018). Materials chemistry and the futurist eco-friendly applications of nanocellulose: Status and prospect. *Journal of Saudi Chemical Society*, 22(8), 949-978.
- Morales, N. J., Candal, R., Famá, L., Goyanes, S., & Rubiolo, G. H. (2015). Improving the physical properties of starch using a new kind of water dispersible nano-hybrid reinforcement. *Carbohydrate Polymers*, 127, 291-299.

- Ochoa-Yepes, O., Di Gioglio, L., Goyanes, S., Mauri, A., & Famá, L. (2019). Influence of process (extrusion/compression molding, casting) and lentil protein content on physicochemical properties of starch films. *Carbohydrate polymers*, 208, 221-231.
- Ochoa-Yepes, O., Medina- Jaramillo, C., Guz, L., & Famá, L. (2018). Biodegradable and Edible Starch Composites with Fiber- Rich Lentil Flour to Use as Food Packaging. *Starch- Stärke*, 70(7-8), 1700222.
- Ogunsona, E., Ojogbo, E., & Mekonnen, T. (2018). Advanced material applications of starch and its derivatives. *European Polymer Journal*, 108, 570-581.
- Pearoval, C., Debeaufort, F., Despera, D., & Voilley, A. (2002). Edible arabinoxylan-based films. 1. Effects of lipid type on water vapor permeability, film structure, and other physical characteristics. *Journal of Agriculture and Food Chemistry*, 50, 3977–3983.
- Pelissari, F. M., Yamashita, F., & Grossmann, M. V. E. (2011). Extrusion parameters related to starch/chitosan active films properties. *International journal of food science & technology*, 46(4), 702-710.
- Pereira Jr, V. A., de Arruda, I. N. Q., & Stefani, R. (2015). Active chitosan/PVA films with anthocyanins from Brassica oleraceae (Red Cabbage) as Time–Temperature Indicators for application in intelligent food packaging. *Food Hydrocolloids*, 43, 180-188.
- Pessanha, K. L. F., Farias, M. G., Carvalho, C. W. P., & Godoy, R. L. D. O. (2018). Starch Films Added of Açaí Pulp (*Euterpe oleracea* Martius). *Brazilian Archives of Biology and Technology*, 61.
- Pratiwi, M., Faridah, D. N., & Lioe, H. N. (2018). Structural changes to starch after acid hydrolysis, debranching, autoclaving- cooling cycles, and heat moisture treatment (HMT): A review. *Starch- Stärke*, 70(1-2), 1700028.

- Pushpadass, H. A., Marx, D. B., & Hanna, M. A. (2008). Effects of extrusion temperature and plasticizers on the physical and functional properties of starch films. *Starch- Stärke*, 60(10), 527-538.
- Qin, Y., Liu, C., Jiang, S., Xiong, L., & Sun, Q. (2016). Characterization of starch nanoparticles prepared by nanoprecipitation: Influence of amylose content and starch type. *Industrial Crops and Products*, 87, 182-190.
- Raigond, P., Sood, A., Kalia, A., Joshi, A., Kaundal, B., Raigond, B., ..., & Chakrabarti, S. K. (2019). Antimicrobial Activity of Potato Starch-Based Active Biodegradable Nanocomposite Films. *Potato Research*, 62(1), 69-83.
- Reis, L. C. B., de Souza, C. O., da Silva, J. B. A., Martins, A. C., Nunes, I. L., & Druzian, J. I. (2015). Active biocomposites of cassava starch: The effect of yerba mate extract and mango pulp as antioxidant additives on the properties and the stability of a packaged product. *Food and Bioproducts Processing*, 94, 382-391.
- Ricco R.A., Wagner M.L., Giberti G.C., & Gurni A.A (1995). Leaf anthocyanins of *Ilex paraguariensis* St. Hil. *Acta Farm Bonaerense*, 14, 87-90.
- Schneider, M., Schneider, R. C., Corbellini, V. A., Mahlmann, C. M., Fior, C. S., & Ferrão, M. F. (2018). Exploratory Analysis Applied for the Evaluation of Yerba Mate Adulteration (*Ilex paraguariensis*). *Food analytical methods*, 11(7), 2035-2041.
- Shahid, M., Islam, S.-u., & Mohammad, F. (2013). Recent advancements in natural dye applications: a review. *Journal of cleaner production*, 53, 310-331.
- Silvestre, C., Duraccio, D., & Cimmino, S. (2011). Food packaging based on polymer nanomaterials. *Progress in polymer science*, 36(12), 1766-1782.
- Silverstein, R. M., Webster, F. X., Kiemle, D. J., & Bryce, D. L. (2014). 531 Spectrometric identification of organic compounds.

- Singleton, V. L., Orthofer, R., & Lamuela-Raventós, R. M. (1999). [14] Analysis of total phenols and other oxidation substrates and antioxidants by means of folin-ciocalteu reagent. In *Methods in enzymology* (Vol. 299, pp. 152-178). Academic press.
- Slavutsky, A. M., Bertuzzi, M. A., Armada, M., García, M. G., & Ochoa, N. A. (2014). Preparation and characterization of montmorillonite/brea gum nanocomposites films. *Food Hydrocolloids*, 35, 270-278.
- Souza, A. H., Corrêa, R. C., Barros, L., Calhelha, R. C., Santos-Buelga, C., Peralta, R. M., ... & Ferreira, I. C. (2015). Phytochemicals and bioactive properties of *Ilex paraguariensis*: An in-vitro comparative study between the whole plant, leaves and stems. *Food Research International*, 78, 286-294.
- Sun, S., Liu, P., Ji, N., Hou, H., & Dong, H. (2017). Effects of low polyhydroxyalkanoate content on the properties of films based on modified starch acquired by extrusion blowing. *Food Hydrocolloids*, 72, 81-89.
- Veiga- Santos, P., Ditchfield, C., & Tadini, C. C. (2011). Development and evaluation of a novel pH indicator biodegradable film based on cassava starch. *Journal of Applied Polymer Science*, 120(2), 1069-1079.
- Vogler, E. A. (1998). Structure and reactivity of water at biomaterial surfaces. *Advances in colloid and interface science*, 74(1-3), 69-117.
- Wang, G. Y., Wang, H. H., Han, Y. W., Xing, T., Ye, K. P., Xu, X. L., & Zhou, G. H. (2017). Evaluation of the spoilage potential of bacteria isolated from chilled chicken in vitro and in situ. *Food microbiology*, 63, 139-146.
- Wang, S., & Copeland, L. (2015). Effect of acid hydrolysis on starch structure and functionality: A review. *Critical reviews in food science and nutrition*, 55(8), 1081-1097.

- Wang, Y. J., Truong, V. D., & Wang, L. (2003). Structures and rheological properties of corn starch as affected by acid hydrolysis. *Carbohydrate Polymers*, 52(3), 327-333.
- Wang, Y. Y., & Ryu, G. H. (2013). Physicochemical and antioxidant properties of extruded corn grits with corn fiber by CO<sub>2</sub> injection extrusion process. *Journal of Cereal Science*, 58(1), 110-116.
- Warren, F. J., Gidley, M. J., & Flanagan, B. M. (2016). Infrared spectroscopy as a tool to characterise starch ordered structure—a joint FTIR–ATR, NMR, XRD and DSC study. *Carbohydrate polymers*, 139, 35-42.
- Yam, K. L., Takhistov, P. T., & Miltz, J. (2005). Intelligent packaging: concepts and applications. *Journal of food science*, 70(1), R1-R10.
- Yoshida, C. M., Maciel, V. B. V., Mendonça, M. E. D., & Franco, T. T. (2014). Chitosan biobased and intelligent films: Monitoring pH variations. *LWT-Food Science and technology*, 55(1), 83-89.
- Yucel, U. (2016). Intelligent Packaging. *Reference Module in Food Science*. Elsevier.



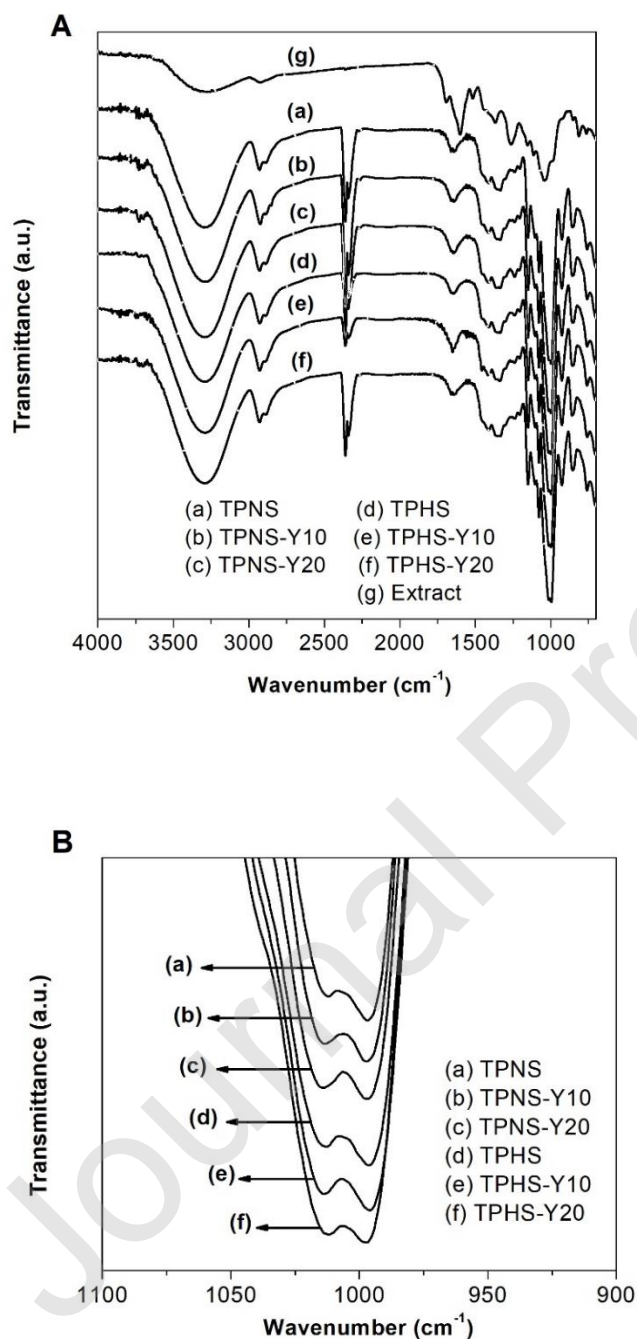


**Figure 1.** (A) FTIR spectra of: a) TPNS, b) TPNS-Y10, c) TPNS-Y20, d) TPHS, e) TPHS-Y10, f) TPHS-Y20 and g) dried yerba mate extract. (B) FTIR in 900-1100  $\text{cm}^{-1}$  region.

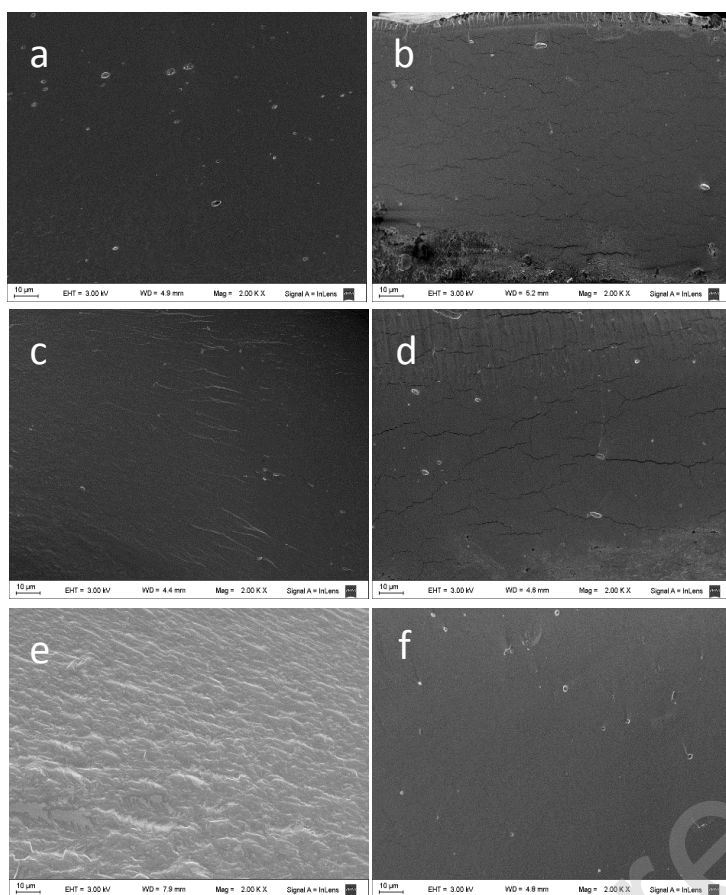


**Figure 2.** Cryogenic fracture surface micrographs (FE-SEM) of the films: a) TPNS, b) TPHS, c) TPNS-Y10, d) TPHS-Y10, e) TPNS-Y20 and f) TPHS-Y20.

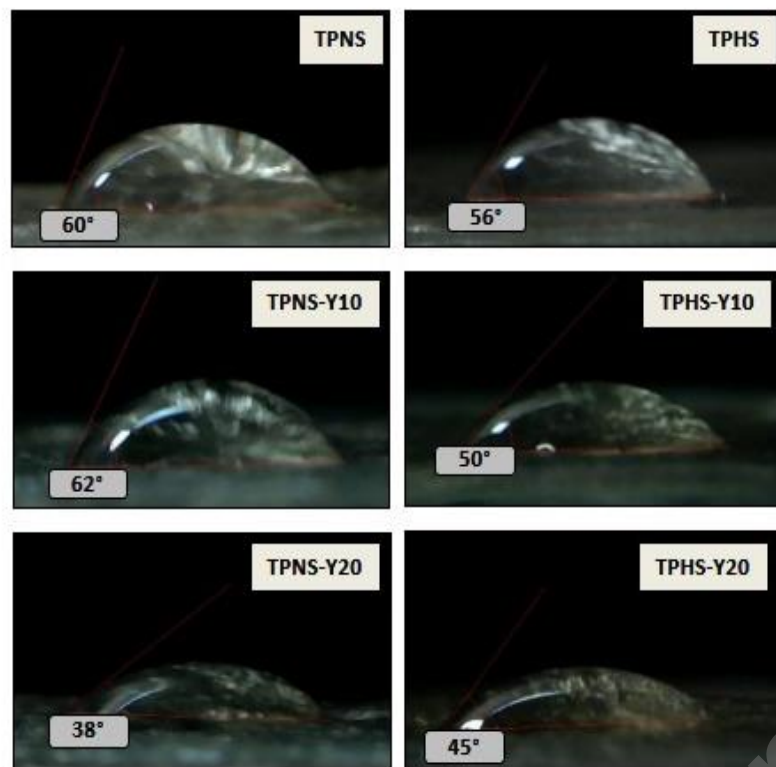


**Figure 3.** Drop of water deposited on the surface of the films and contact angle ( $\theta$ ). The error of the measurements was less than 9% in all cases.

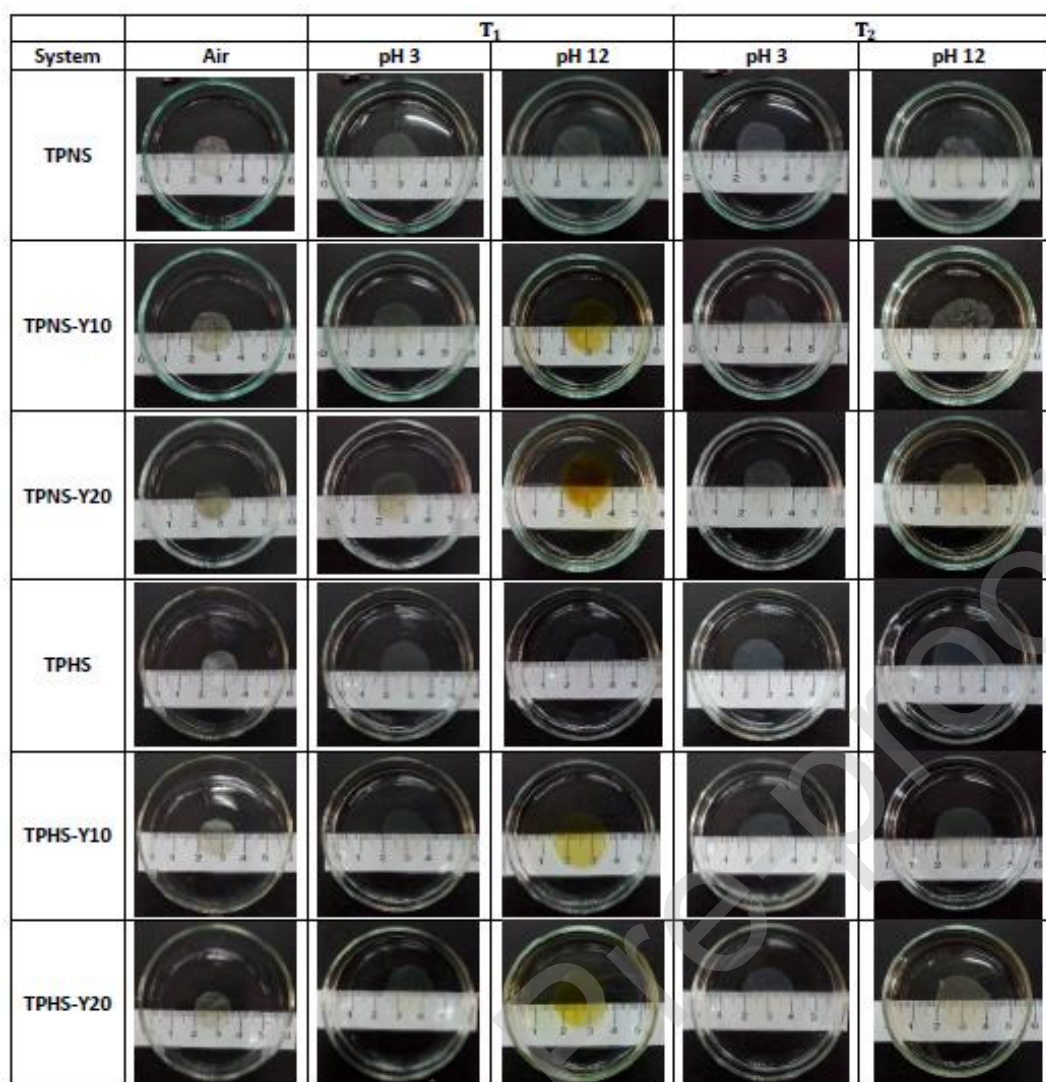


**Figure 4.** Stability at different pH values for all the developed films, 4 min ( $T_1$ ) and 24 h ( $T_2$ ) after immersion.





**Figure 5.** Macroscopic appearance of degradation in soil of all the systems.

**Table 1.** Nomenclature of the films and the concentrations of distilled water and yerba mate extract in the different systems before extrusion.

Nomenclature	Water (wt.%)	Yerba mate extract (wt.%)
TPNS	20	0
TPNS-Y10	10	10
TPNS-Y20	0	20
TPHS	20	0
TPHS-Y10	10	10
TPHS-Y20	0	20

wt. %: percentage of the component's weight/total weight of the system. Weight measurements were determined with an error of less than 1%.

**Table 2.** Total polyphenols content (*TPC*) and antioxidant activity of the films with yerba mate extract in different media.

Samples	<i>TPC</i> (mg GAE/g) [± 0.2]	Antioxidant activity (µM TE/g)		
		Acidic	Hydrophilic	Lipophilic
<b>TPNS-Y10</b>	1.9 <sup>a</sup>	8.8 ± 1.2 <sup>a</sup>	17.9 ± 2.2 <sup>a</sup>	22.3 ± 1.1 <sup>a</sup>
<b>TPNS-Y20</b>	3.6 <sup>b</sup>	15.8 ± 1.8 <sup>b</sup>	29.5 ± 3.1 <sup>b</sup>	44.4 ± 2.5 <sup>b</sup>
<b>TPHS-Y10</b>	1.6 <sup>a</sup>	7.1 ± 0.9 <sup>a</sup>	12.3 ± 2.7 <sup>c</sup>	19.9 ± 2.3 <sup>a</sup>
<b>TPHS-Y20</b>	3.4 <sup>b</sup>	14.5 ± 1.6 <sup>b</sup>	21.6 ± 3.0 <sup>a</sup>	41.7 ± 3.2 <sup>b</sup>

<sup>a,b,c,d</sup> Different letters in the same column indicate significant differences ( $p < 0.05$ ).

**Table 3.** Water vapor permeability (*WVP*), moisture content (*MC*) and water solubility (*S*) of the films.

<b>Film</b>	<b><i>WVP</i> (<math>\times 10^{-10}</math> g/smPa)</b>	<b><i>MC</i> (%) [<math>\pm 1</math>]</b>	<b><i>S</i> (%) [<math>\pm 2</math>]</b>
<b>TPNS</b>	$5.5 \pm 0.5^a$	20 <sup>a</sup>	35 <sup>a</sup>
<b>TPNS-Y10</b>	$4.6 \pm 0.4^a$	22 <sup>a,b</sup>	37 <sup>a,b</sup>
<b>TPNS-Y20</b>	$8.1 \pm 0.5^{b,c}$	22 <sup>a,b</sup>	35 <sup>a</sup>
<b>TPHS</b>	$7.5 \pm 0.8^b$	23 <sup>b</sup>	41 <sup>b,c</sup>
<b>TPHS-Y10</b>	$9.6 \pm 0.8^d$	22 <sup>a,b</sup>	44 <sup>c</sup>
<b>TPHS-Y20</b>	$8.3 \pm 0.6^{c,d}$	21 <sup>a,b</sup>	41 <sup>b,c</sup>

<sup>a,b,c,d</sup> Different letters in the same column represent significant differences ( $p < 0.05$ ).

**Table 4.** Young's modulus (*E*), stress at break ( $\sigma_b$ ), strain at break ( $\epsilon_b$ ), and tensile toughness (*T*) of the developed films.

<b>Film</b>	<b><i>E</i> (MPa)</b>	<b><math>\sigma_b</math> (MPa)</b>	<b><math>\epsilon_b</math> (%)</b>	<b><i>T</i> (MJ m<sup>-3</sup>)</b>
<b>TPNS</b>	$58 \pm 4^a$	$2.8 \pm 0.2^a$	$60 \pm 6^a$	$1.27 \pm 0.12^a$
<b>TPNS-Y10</b>	$63 \pm 3^{a,b}$	$3.0 \pm 0.2^{a,b}$	$65 \pm 4^a$	$1.51 \pm 0.10^b$
<b>TPNS-Y20</b>	$42 \pm 2^c$	$2.9 \pm 0.1^a$	$74 \pm 3^{b,c}$	$1.55 \pm 0.10^b$
<b>TPHS</b>	$50 \pm 3^d$	$3.1 \pm 0.2^{a,b}$	$70 \pm 5^{a,b}$	$1.55 \pm 0.12^b$
<b>TPHS-Y10</b>	$69 \pm 4^b$	$3.2 \pm 0.2^{a,b}$	$63 \pm 5^a$	$1.60 \pm 0.15^b$
<b>TPHS-Y20</b>	$62 \pm 4^{a,b}$	$3.2 \pm 0.1^b$	$80 \pm 3^c$	$2.00 \pm 0.15^c$

<sup>a,b,c</sup> Different letters in the same column represent significant differences ( $P < 0.05$ ).